Journal of Physical Science, Vol. 35(2), 67–84, 2024

# Influence of $TiO_2$ Phases and Operational Parameters on Photocatalytic Degradation of Methyl Orange

Abdul Latif Ahmad,* Jing Yi Chin, Abdul Majeed Alaudin and Norhanis Farhana Mohd Masri

School of Chemical Engineering, Universiti Sains Malaysia, Engineering Campus, 14300 Nibong Tebal, Pulau Pinang, Malaysia

*Corresponding author: chlatif@usm.my

Published online: 31 August 2024

To cite this article: Ahmad, A. L. et al. (2024). Influence of $TiO_2$ phases and operational parameters on photocatalytic degradation of methyl orange. *J. Phys. Sci.*, 35(2), 67–84. https://doi.org/10.21315/jps2024.35.2.5

To link to this article: https://doi.org/10.21315/jps2024.35.2.5

**ABSTRACT:** *In the textile industry, the wastewater produced consists of large amount of dyes. These dyes possess harm to environmental and public health. $TiO_2$ is one of the most common photocatalysts, however studies about degradation efficiency of dye using different phases of $TiO_2$ is scared. Employing photocatalysis, the novelty of this study is to compare methyl orange (MO) degradation efficiency of pure phases of photocatalysts $TiO_2$ (anatase, rutile and brookite) in terms of their photochemical properties and underlying photocatalytic mechanism. Characterisation evaluations including scanning electron microscopy (SEM), fourier-transform infrared spectroscopy (FTIR), X-ray diffraction (XRD) and electrochemical impedance spectroscopy (EIS) were carried out to assess morphology, chemical structure, crystal structure and electron transfer resistance of the photocatalysts. MO adsorption-photocatalysis removal percentage by pure phase $TiO_2$, which are anatase, brookite and rutile were attained at 57%, 48% and 19%, respectively. The main reason that contributes to high degradation rate of MO by $TiO_2$-anatase could be due to the good dye-photocatalyst affinity and the least electron transfer resistance. Besides, other affecting parameters such as initial concentration of photocatalyst, initial concentration of dye and pH of the dye solution were evaluated. It was found that photocatalytic efficiency was enhanced with increasing initial concentration of photocatalyst from 0.25 mg/mL to 1 mg/mL (degradation improved from 50% to 80%), with decreasing initial dye concentration and under acidic condition.*

**Keywords:** photocatalysis, $TiO_2$, methyl orange, dye, degradation

## 1. INTRODUCTION

The wastewater that involved dyes is a very serious issue. Globally, it is estimated that 700,000 tons of different types of dyes are being released.[1] The released dyes have been classified into various categories, including azo dyes, direct dyes, basic dyes, vat dyes and others. One of the most widely used types of azo dyes is reactive dye.[2] Due to the colour brightness, and simple application, reactive dye is used in textile industries extensively. These dyes released into the water bodies are very toxic and possess negative effects to the living organism. These dyes are highly colored substances and will inhibit sunlight from penetrating the aqueous body.[3]

To protect the environment, various wastewater treatment technologies for dyes removal were introduced, such as coagulation, filtration, adsorption, sedimentation and membrane technologies.[4] However, all these methods have their own drawbacks such as involvement of additional chemicals or large quantities of energy, and the creation of waste and byproducts.[5] Therefore, it is important to encourage the development of more sustainable water treatment technology to ensure the quality of the water.

Photocatalysis has been getting a lot of research attention recently.[6] That is because, ideally, this technique does not produce secondary waste products. Photocatalysis is a process that can destroy or degrade toxic compounds by oxidative or reductive mechanism with the presence of photocatalyst. This process is very efficient, can operate under atmospheric temperature and pressure. Semiconductors like titanium dioxide ($TiO_2$), zinc oxide (ZnO), tungsten (IV) oxide ($WO_3$) and others have been effective at converting a variety of potentially refractory organics into quickly biodegradable compounds, eventually mineralising them to harmless carbon dioxide and water. Each photocatalyst has a different gap energy and different oxidising power. In research and development of photocatalysis technology, $TiO_2$ has attracted the most interest among semiconductor catalysts.

$TiO_2$ photocatalyst has been actively studied to improve the photocatalytic degradation of dyes. Several studies report the significance of operational parameters that influence the efficiency of photocatalytic degradation. Some basic parameters are phases of photocatalysts, concentration of substrates, concentration of photocatalyst, pH of the solution and others. Saquib and Muneer observed that under the existence of pure anatase $TiO_2$, the mineralisation and degradation of dye is faster compared to another phase of $TiO_2$ photocatalysts.[7] Gnanaprakasam et al. observed that increasing the initial concentration of dyes caused the efficiency of photocatalysis degradation to reduce due to reduction of the light path length

of the photons thus reducing photocatalytic efficiency.[8] Toor et al. also reported that pH is one of the parameters that influence the characteristics of textile waste and the generation of hydroxyl radicals.[9] In acidic pH, the rate of degradation increases while in basic pH, degradation rate decreases.

Gathering the information, the objectives of this study are to investigate the effect of different phases of $TiO_2$, initial concentration of photocatalyst, initial concentration of dye, and pH of solution towards efficiency of photocatalytic degradation of methyl orange (MO). MO is chosen in this study because it is a widely used azo dye in textile industries, and it has easily measurable absorption spectrum for accurate evaluation of photocatalytic activities.

## 2. MATERIALS AND METHODOLOGY

### 2.1 Materials and Characterisations of Photocatalysts

Three phases of commercial $TiO_2$ (anatase, rutile and brookite) obtained from Sigma-Aldrich (USA) were the photocatalysts used to degrade dyes. Methyl orange (Sigma-Aldrich, USA) was used as pollutant model to study the affecting parameters of photocatalytic degradation. To characterise the chemical bonding, crystal structure and morphology of $TiO_2$, the following experimental procedures were conducted. The chemical bonding of $TiO_2$ was determined using an attenuated total reflection-fourier transform infrared (ATR-FTIR) spectrometer (Nicolet iS10, USA). For crystal structure analysis, X-ray diffraction (XRD) was performed using a Bruker D8 Phaser. The scanning was conducted at a rate of 2° per min with 0.02° intervals and a counting time of 1 s per step, employing a Cu-Kα radiation source. To observe the morphologies of $TiO_2$, scanning electron microscopy (SEM) was utilised, specifically the extreme high resolution field emission scanning electron microscope (XHR-FESEM, Model FEI Verios 460L). These techniques collectively provide detailed information on the structural and morphological characteristics of the $TiO_2$ samples.

The electrochemical impedance spectroscopy (EIS) of the photocatalysts was examined using a portable bipotentiostat/galvanostat/impedance analyser μStat-i400 (DropSens, Asturias, Spain). A conventional three-electrode system was employed, consisting of a platinum wire as the counter electrode, a saturated Ag/AgCl (3 M KCl) electrode as the reference electrode, and a modified carbon working electrode. To prepare the working electrode, 0.5 mg of each photocatalyst was dispersed in a mixture containing 0.1 mL Nafion and 0.9 mL ethanol. Subsequently, 10 μL of the slurry was dropped-casted onto the surface of the carbon working electrode and allowed to air dry overnight. For EIS

testing, the three electrodes (counter, working and reference) were immersed in a 0.1 M KCl solution containing 5 mM of hexaaammineruthenium (III) chloride (Sigma-Aldrich, USA).

## 2.2 Degradation of Dyes by Photocatalysts

To investigate the degradation of MO using three $TiO_2$ phases (anatase, rutile and brookite), an experimental procedure was conducted as follows: an initial MO concentration of 5 ppm was prepared, and $TiO_2$ was added at a concentration of 1 mg/mL. The mixture was then stirred in a black box for 2 h to achieve adsorption-desorption equilibrium. Following this equilibration period in the dark, the light source (fluorescent light with 18W × 4 bulbs) was switched on to initiate the photocatalytic process. Samples of 1 mL were collected every hour and filtered through a 0.45 μm cellulose acetate syringe filter. The concentration of MO in these samples was determined using UV-Vis spectrophotometry at a wavelength of 460 nm. This procedure was repeated for each $TiO_2$ phase (anatase, rutile and brookite) to compare their photocatalytic efficiencies in degrading MO. Degradation efficiency of MO was calculated based on Equation 1:

$$\text{Degradation efficiency (\%)} = \left( \frac{C_o - C_t}{C_o} \right) \times 100\% \quad (1)$$

whereby $C_0$ is the initial concentration of MO while $C_t$ is the final concentration of MO. Degradation kinetics of the photocatalytic process was calculated using the following equation:[10, 11]

$$\ln \left( \frac{C_t}{C_o} \right) = -kt \quad (2)$$

whereby $C_t$ denotes concentration of dyes at time (t), $C_o$ represents the initial dyes concentration and k is the degradation kinetic.

For the effect of initial photocatalyst concentration evaluation, the aforementioned steps were repeated by using the best $TiO_2$ phase. The concentration of dye was fixed at 5 ppm while the initial concentration of photocatalyst was altered by introducing 2.5 mg, 7.5 mg, 5 mg and 10 mg of $TiO_2$ in 10 mL of dye solution. The concentration range of $TiO_2$ was chosen based on literature that identified optimal concentration for photocatalytic processes.[12] The range selected ensures that there is an adequate amount of photocatalyst to generate reactive species while avoiding excessive aggregation. Next, evaluation of influence of initial concentration of MO was conducted by fixing the concentration of $TiO_2$ at 1 mg/mL, while altering concentration of MO at 5 ppm, 10 pmm, 15 ppm and 20 ppm. Lastly, the effect of different pH to degrade dye studied at pH 2, 4, 6,

8 and 10. Acidic and alkaline solution was attained by adjusting the pH using sulfuric acid ($H_2SO_4$) and sodium hydroxide (NaOH). The MO photodegradation steps as mentioned above were repeated in the scavenger tests. During the test, 10 mM of ethanol, isopropanol alcohol (IPA), triethanolamine (TEOA) and ascorbic acid (AA) were added into each of the MO solution at the beginning of the experiment.

## 3. RESULTS AND DISCUSSION

The SEM micrographs of $TiO_2$ nanoparticle for anatase, rutile and brookite are shown in Figure 1. From Figure 1 (a) and (d), the morphology of anatase nanoparticle showed agglomeration. The agglomeration occurs because the anatase is unstable, so they tend to join with each other until they are relatively stable.[13] Based on Figure 1 (b) and (e), the morphology of rutile is similar to anatase, but the particle size of anatase is smaller than rutile. Hence, the surface area of anatase is higher as compared to rutile. Furthermore, brookite occurs as cluster of crystals, as shown in Figure 1 (c) and (f). Brookite is also observed as overgrowths on detrital titanium oxide grams where the brookite rhombs are elongated and extend on both sides of the oxide core.[14]

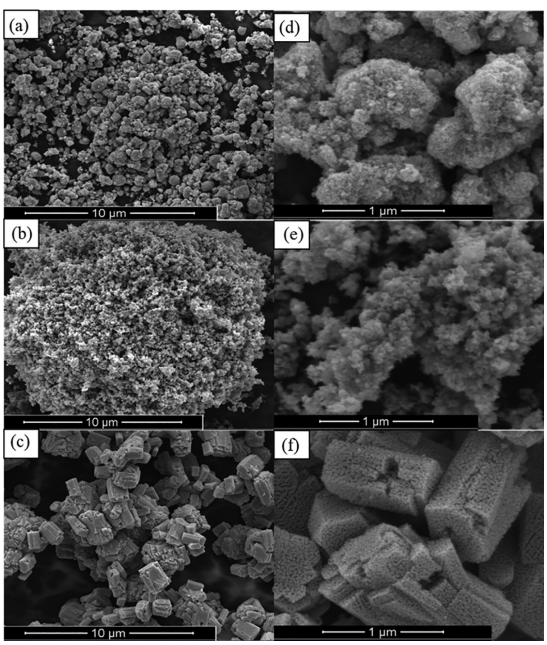


Figure 1: SEM micrographs (10 µm magnification) of (a) anatase, (b) rutile, (c) brookite and magnified (1 µm magnification) SEM images of (d) anatase, (e) rutile, and (f) brookite.

The chemical bond of the $TiO_2$ was then investigated using FTIR spectroscopy. From Figure 2, it could be observed that all three $TiO_2$ photocatalysts namely anatase, brookite and rutile had peaks at similar wavenumbers, meaning they had similar molecular structures. Figure 2 shows the FTIR spectra versus the transmittance for $TiO_2$-anatase, $TiO_2$-brookite and $TiO_2$-rutile nanoparticles (region 3,650 $cm^{-1}$–650 $cm^{-1}$). The spectra peaks in the region 1,150 $cm^{-1}$–500 $cm^{-1}$ are attributed to Ti–O and/or Ti–O–Ti bonds.[15]

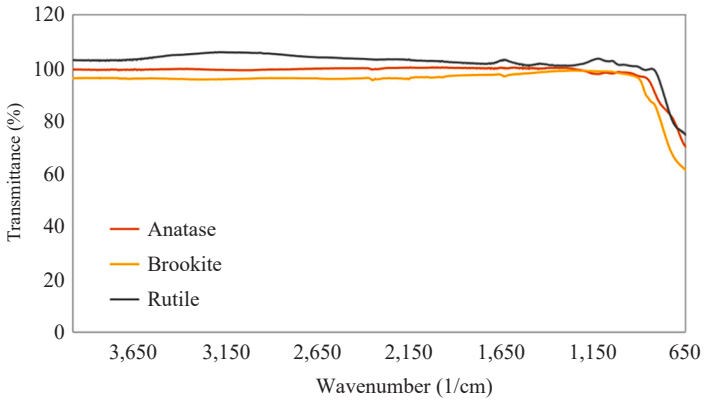


Figure 2: FTIR spectra of $TiO_2$-anatase, brookite and rutile nanoparticles.

As the FTIR analysis could not provide information about the differences between the three phases of $TiO_2$ due to their similar chemical bonds, XRD analysis was performed to investigate the differences of their crystal structures. Figure 3 indicates the XRD pattern of $TiO_2$-anatase, $TiO_2$-brookite and $TiO_2$-rutile. The XRD peaks are strong, indicating all samples have high crystallinity.

According to the standard JCPDF card no. 73-1764, the XRD peaks matched the tetragonal crystal system of anatase [space group: I41/amd (141); a = b = 0.377 nm, c = 0.948 nm].[16] Besides, the XRD peaks also corresponded to orthorhombic crystal system of brookite [space group: Pbca (61); a = 0.919 nm, b = 0.546 nm, c = 0.515 nm] and tetragonal crystal system of rutile [space group: P42/mnm (136); a = b = 0.458 nm, c = 0.295 nm].

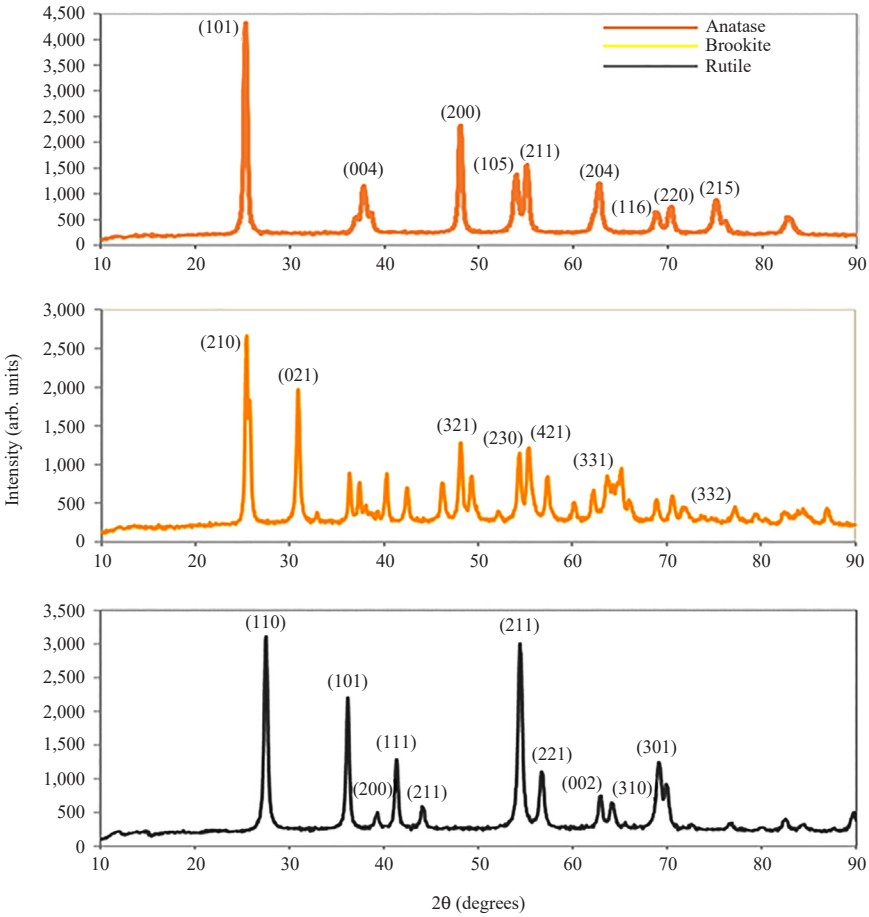


Figure 3: XRD patterns of $TiO_2$-anatase, $TiO_2$-brookite and $TiO_2$-rutile.

As mentioned, all the diffraction peaks identified were correlated to the characteristics of $TiO_2$-anatase, $TiO_2$-brookite and $TiO_2$-rutile. For instance, the peaks observed at 2θ values of ~25.05°, 37.9°, 48.1°, 54.1°, 55.1°, 62.7°, 68.7°, 70.1° and 75.1° for the top diffraction pattern indicate the (101), (004), (200), (105), (211), (204), (116), (220) and (215) lattice planes, respectively, indicating a pure and highly crystalline $TiO_2$ in its anatase phase. The diffraction peaks of brookite are presence at ~25.26°, 34.9°, 54.1°, 55.1°, 62.7°, 68.9° and 75.3° for the top diffraction pattern indicating the (210), (021), (321), (230), (421), (331) and (332) lattice planes, respectively, matching the crystalline $TiO_2$-brookite phase. The planes of brookite are in orthorhombic structure. While for rutile, the diffraction peaks presence at ~27.5°, 36.2°, 39.3°, 41.4°, 44.0°, 54.3°, 56.5°, 62.7°, 63.9° and 69.8° indicate the (110), (101), (200), (111), (210), (211), (002),

(310) and (301) lattice planes, respectively.[17] For all three phases of $TiO_2$, no extra peaks were detected, indicating no impurities and other structural phases. This proves that all the three $TiO_2$ samples are of high purity and crystallinity.

Additionally, EIS studies of the pure phases of $TiO_2$ which are anatase, rutile and brookite were carried out to evaluate the resistance against electron transfer during the photocatalytic activation process. The Nyquist plots for $TiO_2$ studied were presented in Figure 4. Generally, the arcs of the EIS Nyquist plots are attributed to the charge transfer impedance. Smaller arc indicates smaller electron transfer resistance.[18]

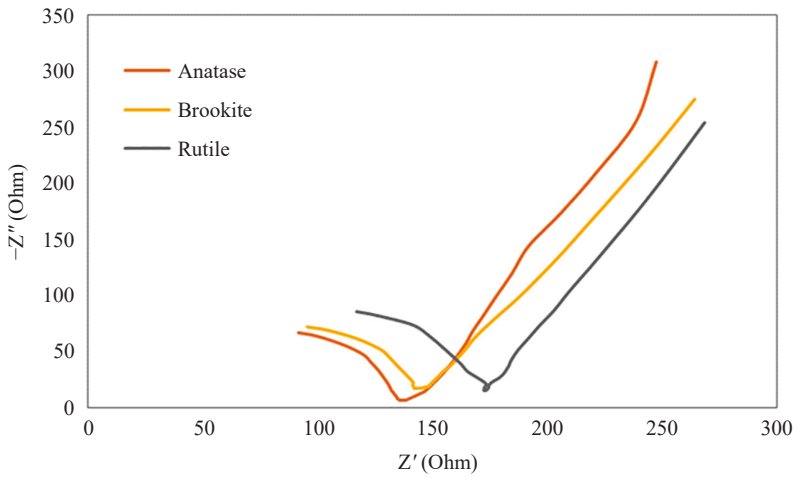


Figure 4: EIS of anatase, rutile and $TiO_2$-brookite.

As depicted in Figure 4, anatase had the smallest arc radius, while rutile had the biggest arc radius. The smaller arc radius of anatase indicates separation of photogenerated carriers will be improved for effective photocatalytic degradation process.[19] Besides, anatase is expected to have the most effective separation and migration of electron-hole pairs as compared to brookite and rutile.[20] Therefore, it was predicted that anatase would result in the best photocatalytic degradation efficiency out of the three $TiO_2$ phases.

Degradation efficiencies of anatase, brookite and rutile of $TiO_2$ were evaluated using MO as pollutant model. As reported in Figure 5, $TiO_2$-anatase had the best MO degradation efficiency at 57.8% than $TiO_2$-brookite (28.81%) and $TiO_2$-rutile (18.19%).

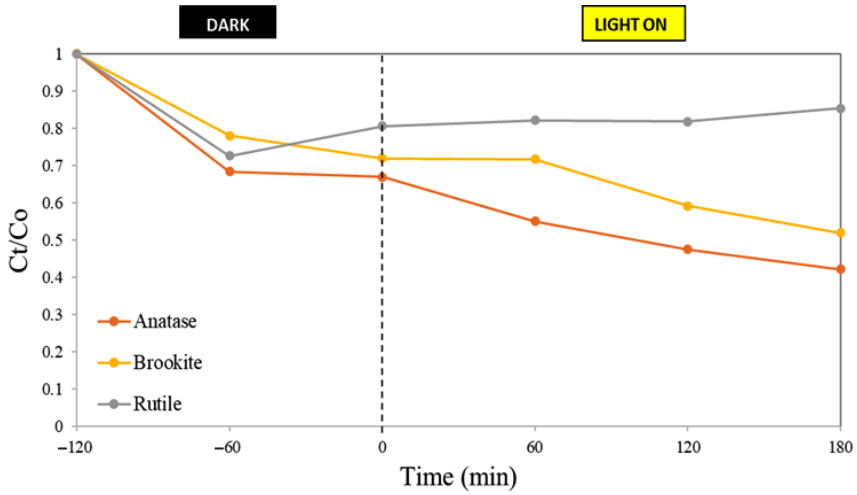


Figure 5: Degradation efficiency of MO using anatase, rutile and $TiO_2$-brookite.

Several factors have contributed to high $TiO_2$-anatase degradation efficiency. Anatase has better photocatalytic degradation compared to brookite and rutile due to the higher surface area that provides more active sites, which can enhance the adsorption of organic molecules like MO, subsequently lead to more efficient chemical reactions. Besides, anatase is more efficient in generating reactive oxygen species (ROS), such as hydroxyl radicals (·OH), when exposed to light.[21] These ROS play a crucial role in the degradation of organic pollutants by oxidising them into smaller, less harmful molecules. The higher generation of ROS in anatase enhances its degradation capability.[22] Lastly, anatase has a less thermodynamically stable crystal structure compared to brookite and rutile.[23] This structural characteristic of anatase contributes to easier surface reactions and provides better accessibility for reactants like MO molecules to reach the active sites on the surface of anatase.[24] Hence, degradation activity of MO would be enhanced due to anatase's higher reactivity, facilitating more electron-hole pairs (reactive species) generation and separation. The reactive species attack and degrade the MO molecules.[24]

Degradation kinetics could evaluate how fast the photocatalysts could degrade MO as compared to the other photocatalysts studied. Hence, besides determining the final MO degradation percentage, degradation kinetic is also an essential factor to be investigated. Using the first-order kinetic model, MO's degradation rate constants (k) were derived from the degradation graphs. The k values for anatase, brookite and rutile were 0.0027 $min^{-1}$, 0.0016 $min^{-1}$ and 0.0003 $min^{-1}$, respectively as shown in Figure 6.

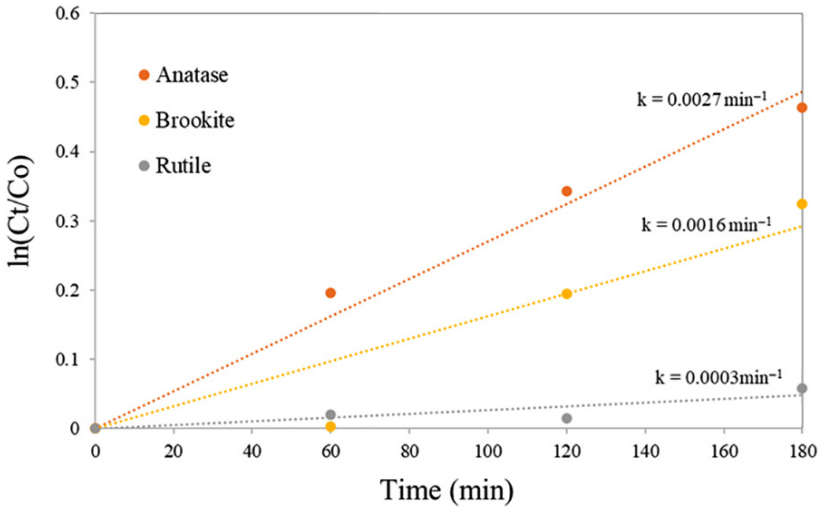


Figure 6: Degradation kinetics of MO by $TiO_2$ (anatase, rutile and brookite).

The kinetics of anatase was the most intense as compared to brookite and rutile. In short, the photocatalytic activities of the photocatalysts are anatase > brookite > rutile. This result is highly correlated to the electron transfer resistance in the photocatalysts. $TiO_2$-anatase has the lowest electron transfer resistance among all, as evaluated in the EIS analysis. Hence, it has the most efficient electron-hole pairs separation and migration across the photocatalyst band gap. Thus, radical species could be generated more effectively to facilitate the photocatalytic degradation of MO.

Active species involved in photodegradation of MO were investigated by carrying out scavenger studies. $TiO_2$-anatase, which provided the best photocatalytic degradation efficiency, was used in this scavenger study. To quench the active species, different scavengers were used. As shown in Figure 7, IPA, AA, TEOA and ethanol were used to scavenge ·OH, superoxide radical (·$O_2^-$), holes ($h^+$) and electron ($e^-$), respectively.

AA and ethanol affected the photodegradation of MO slightly, indicating ·$O_2^-$ and $e^-$ active species were not dominant in the photocatalytic activity of MO. On the other hand, under the existence of IPA, degradation rate of MO decreased significantly. This result implies that ·OH radical species played a significant role in degrading MO. Furthermore, TEOA suppressed the photocatalytic activity completely, showing that $h^+$ is the dominant radical species in degrading MO.

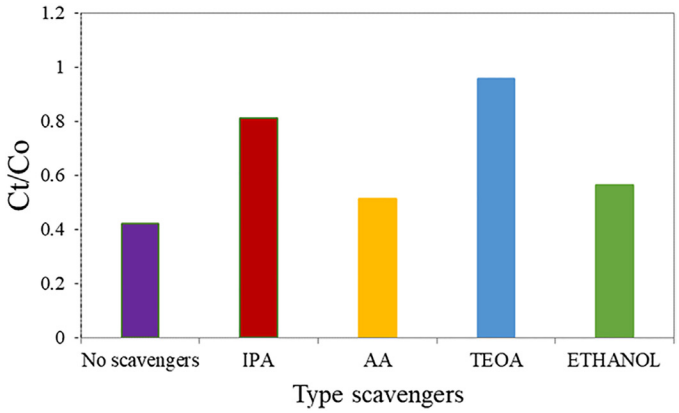


Figure 7: Radical scavengers' study of MO degradation using $TiO_2$-anatase under visible light irradiation.

The second affecting parameter evaluated was the effect of different initial photocatalyst concentration. MO acted as the pollutant model in this parameter study. $TiO_2$-anatase was used in this parameter study as it was determined to be the best $TiO_2$ phase to degrade MO. The quantity of photocatalyst has an impact on dye degradation as well. Figure 8 shows the effect of initial photocatalyst dose on the photodegradation of MO. An increased photocatalyst dose from 2.5 mg to 10 mg leading to enhanced photocatalytic activity drastically, due to the easier and higher number of radical species formation on the photocatalyst surface. The rate of degradation of MO was 0.001993 mg/L·min, 0.005696 mg/L·min, 0.0011356 mg/L·min and 0.013448 mg/L·min for 2.5 mg, 5 mg, 7.5 mg and 10 mg of anatase, respectively. The increase in the degradation rate and percentage of decolourisation could be attributed to the increase in the number of active sites on the $TiO_2$-anatase surface with the increasing concentration. Hence, more MO molecules could be adsorbed on the photocatalyst and promoted enhanced photocatalytic activity. By increasing the dosage of $TiO_2$-anatase, the number of free radicals (·OH and $O_2^-$) in solution are also increased, consequently leading to improved photodegradation of the MO. Hence, the rate of dye photodegradation rises as photocatalyst concentration rises. However, there is a limitation at which further increment of photocatalyst concentration (from 7.5 mg to 10 mg photocatalyst) would deteriorate the degradation efficiency.[25] This is because beyond a certain photocatalyst concentration, the solution gets unclear and inhibits light radiation, which prevents the reaction from continuing and lowers the percentage of decolourisation.[26]

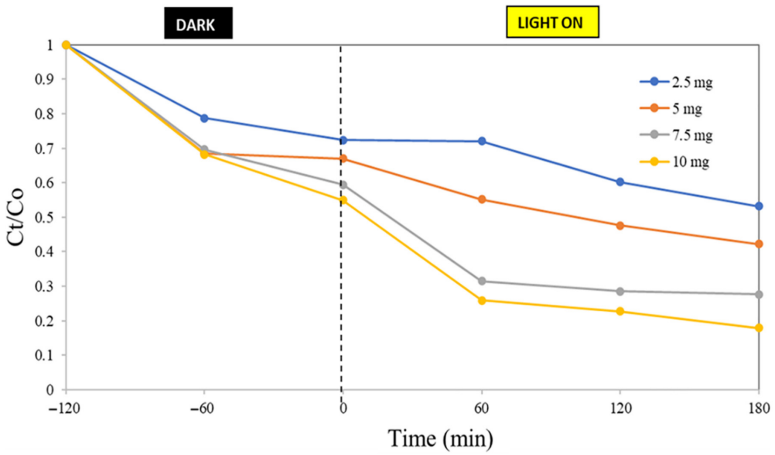


Figure 8: Degradation efficiency of MO using different concentration of $TiO_2$-anatase.

Based on Figure 9, the k value of 10 mg initial photocatalyst concentration was the highest among all. Therefore, the photocatalytic activity of the samples was under the order of 10 mg > 7.5 mg > 5 mg > 2.5 mg. This result demonstrated relevancy to the number of available active sites for photocatalytic degradation. Due to the highest number of photocatalytic sites, 10 mg anatase degraded MO in the highest rate while 2.5 ppm has the lowest degradation kinetic rate due to limited photocatalytic sites.

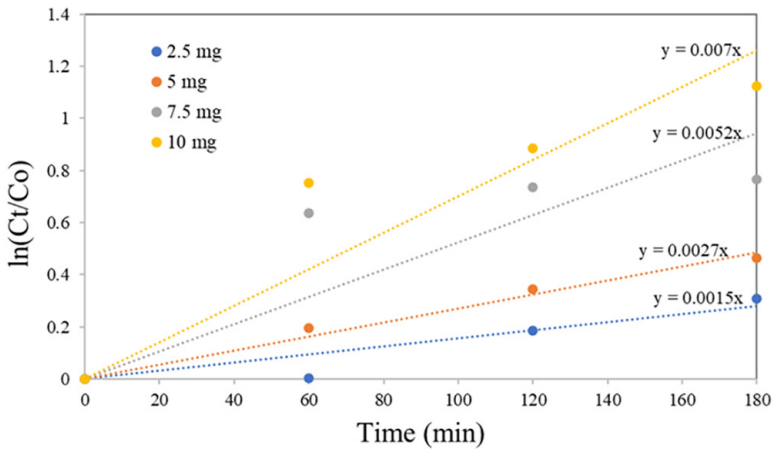


Figure 9: Degradation kinetics of MO by using different concentration of $TiO_2$-anatase.

While fixing the amount of photocatalyst, the concentration of the dye is expected to influence the degradation efficiency. Similar to the previous parameter, $TiO_2$-anatase was used in this investigation. In Figure 10, MO with initial concentration from 5 ppm to 20 ppm were degraded using $TiO_2$-anatase. The highest degradation efficiency, 70.51%, was attained by the lowest initial MO concentration studied (5 ppm). Degradation efficiency reduced was lowered following the increment of the initial MO concentration up to 20 ppm.

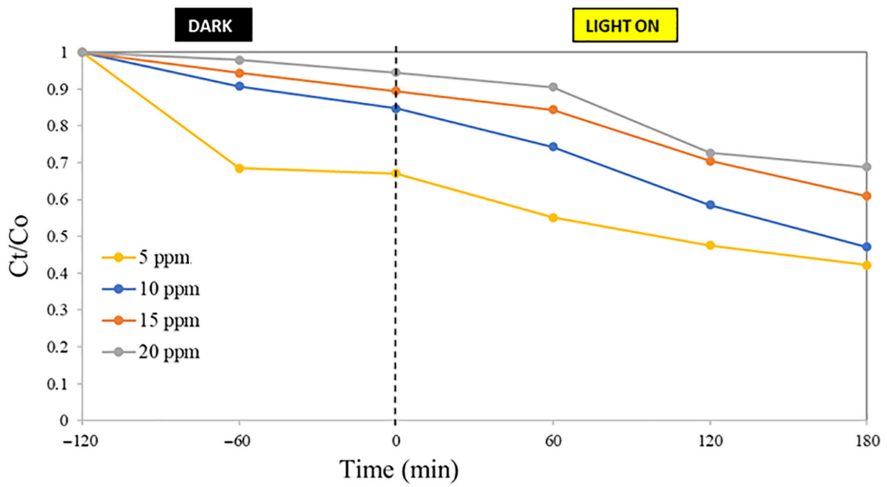


Figure 10: Degradation efficiency of MO under different initial MO concentrations.

When initial MO concentration was low, there were excessive photocatalytic sites available for the dye to adsorb on the photocatalyst and undergo degradation. As the number of MO molecules increased, they would compete for the limited photocatalytic sites. Hence, degradation efficiency would be reduced. Apart from lowering degradation efficiency, a lower k value was also observed when concentration of MO increases. Another contributing factor towards this reduction is that the abundant MO molecules would hinder light penetration to the photocatalyst surface, suppressing the formation of radical species. Besides, when more MO molecules were adsorbed on the photocatalyst surface, it could also block the photons from reaching the surface of the photocatalyst. As a result, electrons in the photocatalyst could not be excited effectively, thus lesser decolourisation was accomplished.[27] This result is coherent to study conducted Zhu et al. at which increasing the initial MO concentration decreased the amount of photons entering the solutions to carry out degradation activity.[28] Degradation kinetics of different MO concentration solutions were again evaluated. Following the degradation trend in Figure 10, as expected, the k value of 5 ppm initial dye concentration was the highest among all (see Figure 11).

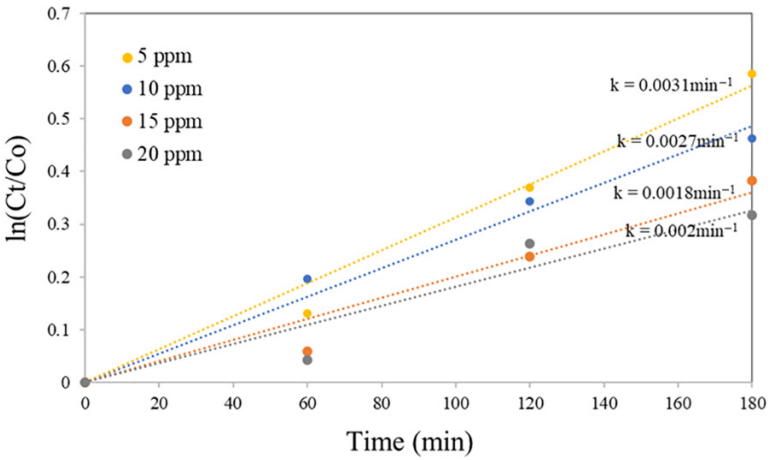


Figure 11: Degradation kinetics of MO under different dye concentration.

Moreover, the efficacies of photocatalytic processes would be highly influenced by pH. From Figure 12, it can be seen that under acidic conditions (pH 2 and 4), MO was being degraded more efficiently than the original pH condition (pH 6). At pH 2 and 4, the amount of MO adsorbed on $TiO_2$ was similar but based on the value k in Figure 13, MO solution at pH 2 has higher degradation kinetic than pH 4. So that means the photocatalytic degradation rate for pH 2 is higher.

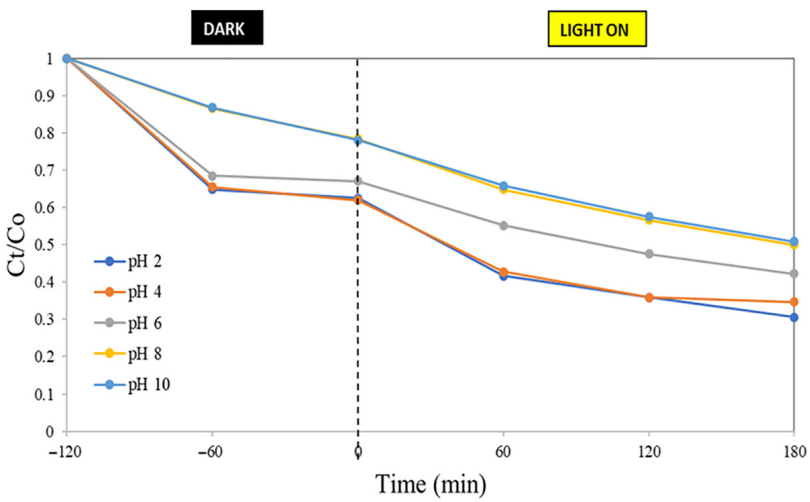


Figure 12: Removal of MO by using $TiO_2$-anatase under different initial pH.

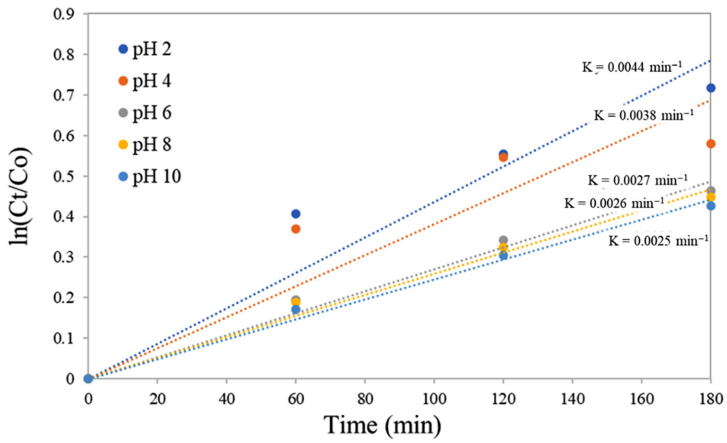


Figure 13: Degradation kinetics of MO by using $TiO_2$-anatase under different initial pH.

This is because at pH 2, the concentration of $H^+$ in the solution is significantly higher, resulting in a more acidic environment compared to pH 4. The increased concentration of $H^+$ ions at pH 2 leads to the protonation of the surface hydroxyl groups of $TiO_2$, resulting in the formation of positively charged surface species, such as $TiOH_2^+$ or $TiOH_3^+$. On the other hand, under acidic conditions, MO (an anionic dye) will be negatively charged. Hence, adsorption between the protonated surface species of $TiO_2$ and negatively charged MO will be enhanced. Additionally, the higher concentration of $H^+$ ions can also generate more ROS like ·OH on the surface of $TiO_2$, which further accelerates the degradation reactions. At pH 4, the concentration of $H^+$ ions were lower compared to pH 2. This reduced acidity results in fewer protonated surface species and a lower concentration of ROS, leading to a slightly lower degradation rate compared to pH 2. Another reason for a fast degradation of MO in acidic condition is the structural change of MO in acidic condition. The quinoid structure of MO (acidic condition) has a relatively lower bond energy. This renders MO to be degraded more easily.

While for the alkali pH which were 8 and 10, a similar percentage of MO was adsorbed on the photocatalyst, but pH 8 has higher degradation rate compared to 10. This is because pH 10 is more alkaline compared to 8. Under highly alkaline conditions (pH 10), $TiO_2$ can undergo surface deactivation or structural changes that can limit its photocatalytic activity. Alkaline conditions may lead to the formation of titanium hydroxides or other species that hinder the photocatalytic degradation process.[29] At higher pH values, the concentration of hydroxyl ions ($OH^-$) in the solution increases. These $OH^-$ compete with the pollutants for reaction with the photogenerated $h^+$ on the $TiO_2$ surface, reducing the availability of $h^+$ for pollutant degradation.[29] As a result, the degradation rate decreases under more basic pH.

## 4. CONCLUSION

The properties of different phases of photocatalyst ($TiO_2$) were analysed and their efficacy to degrade MO were contrasted. The MO removal efficiency followed the order of $TiO_2$-anatase (57.81%) > TiO2-brookite (48.81%) > $TiO_2$-rutile (18.91%). The reason could be due to good adsorption between MO and $TiO_2$-anatase. Adsorption is a requirement for photocatalytic degradation, which attracts a MO towards the photocatalyst surface and starts the degradation activity. Since MO has an affinity for the photocatalysts (in this study, anatase > brookite > rutile), MO can be effectively removed. The scavenging test concluded that ·OH and $h^+$ are two major radical species that are involved in the MO degradation by $TiO_2$-anatase. Several parameters that will affect dye degradation efficiency were also studied. Under different initial photocatalysts concentrations, increasing the dosage of $TiO_2$-anatase, the number of free radicals (·OH and $O_2^-$) in solution are also increased consequently leading to enhanced photodegradation of the MO. On the contrary, low initial concentration of MO dye will lead to better degradation efficiency. This is because at low dye concentration, less competition occurred for the active site of the photocatalyst. Lastly, the highest degradation between photocatalyst and MO is at acidic solution. At pH 2, the concentration of $H^+$ in the solution is higher and caused MO (negatively charged) to be adsorbed electrostatically more efficiently due to its attraction with the positively charged $TiO_2$-anatase surface.

## 5. ACKNOWLEDGEMENTS

This work was supported by the Long-Term Research Grant Scheme (LRGS/1/2018/USM/01/1/4), Ministry of Higher Education Malaysia.

## 6. REFERENCES

1. Chandanshive, V. et al. (2020). *In situ* textile wastewater treatment in high rate transpiration system furrows planted with aquatic macrophytes and floating phytobeds. *Chemosphere*, 252, 126513. https://doi.org/10.1016/j.chemosphere.2020.126513
2. Ayed, L. et al. (2011). Decolorization and degradation of azo dye Methyl Red by an isolated Sphingomonas paucimobilis: Biotoxicity and metabolites characterization. *Desalination*, 274(1–3), 272–277. https://doi.org/10.1016/j.desal.2011.02.024
3. Carney Almroth, B. et al. (2021). Assessing the effects of textile leachates in fish using multiple testing methods: From gene expression to behavior. *Ecotox. Environ. Safe*, 207 111523. https://doi.org/10.1016/j.ecoenv.2020.111523

4. Saiz, J., Bringas, E. & Ortiz, I. (2014). New functionalized magnetic materials for As5+ removal: Adsorbent regeneration and reuse. *Ind. Eng. Chem. Res.*, 53(49), 18928–18934. https://doi.org/10.1021/ie500912k
5. Rivero, M. J. et al. (2014). Kinetic analysis and biodegradability of the Fenton mineralization of bisphenol A. *J. Chem. Technol. Biotechnol.*, 89(8), 1228–1234. https://doi.org/10.1002/jctb.4376
6. Chong, M. N. et al. (2010). Recent developments in photocatalytic water treatment technology: A review. *Water Res.*, 44, 2997–3027. https://doi.org/10.1016/j.watres.2010.02.039
7. Saquib, M. & Muneer, M. (2003). $TiO_2$-mediated photocatalytic degradation of a triphenylmethane dye (gentian violet), in aqueous suspensions. *Dyes Pigment*, 56(1), 37–49. https://doi.org/10.1016/S0143-7208(02)00101-8
8. Gnanaprakasam, A., Sivakumar, V. M. & Thirumarimurugan, M. (2015). Influencing parameters in the photocatalytic degradation of organic effluent via nanometal oxide catalyst: A review. *Indian J. Eng. Mater. Sci.*, 2015, 601827. https://doi.org/10.1155/2015/601827
9. Toor, A. P. et al. (2006). Photocatalytic degradation of Direct Yellow 12 dye using UV/$TiO_2$ in a shallow pond slurry reactor. *Dyes Pigment*, 68(1), 53–60. https://doi.org/10.1016/j.dyepig.2004.12.009
10. Jasni, N. et al. (2023). Photodegradation of oxytetracycline using fluorescent light driven ZnO quantum dots synthesised via microwave method. *J. Phys. Sci.*, 34(1), 27–41. https://doi.org/10.21315/jps2023.34.1.3
11. Mahi, K. & Mostefa, R. (2021). Structural and optical properties of $MAl_2O_4$ spinel-type prepared by solution combustion synthesis method for photocatalytic application. *J. Phys. Sci.*, 32(3), 61–73. https://doi.org/10.21315/jps2021.32.3.5
12. Khojasteh, H. et al. (2024). Optimization of $Fe_3O_4$@$SiO_2$/Ag/AgCl/CdS nanocomposite via response surface methodology: An efficient visible-light photocatalyst for methyl orange degradation. *J. Sol-Gel Sci. Technol.*, 111, 362–380. https://doi.org/10.1007/s10971-024-06458-x
13. Nasikhudin, et al. (2018). Study on photocatalytic properties of $TiO_2$ nanoparticle in various pH condition. *J. Phys. Conf. Ser.*, 1011(1), 012069. https://doi.org/10.1088/1742-6596/1011/1/012069
14. Morad, S. (1986). SEM study of authigenic rutile, anatase and brookite in Proterozoic sandstones from Sweden. *Sediment. Geol.*, 46(1–2), 77–89. https://doi.org/10.1016/0037-0738(86)90007-2
15. Verma, R., Gangwar, J. & Srivastava, A. (2017). Multiphase $TiO_2$ nanostructures: A review of efficient synthesis, growth mechanism, probing capabilities, and applications in bio-safety and health. *RSC Adv.*, 70(7), 44199–44224. https://doi.org/10.1039/C7RA06925A
16. Eddy, D. R. et al. (2024). Study on triphase of polymorphs $TiO_2$ (anatase/rutile/brookite) for boosting photocatalytic activity of metformin degradation. *Chemosphere*, 351, 141206. https://doi.org/10.1016/j.chemosphere.2024.141206
17. Wang, Y. et al. (2015). New insights into fluorinated $TiO_2$ (brookite, anatase and rutile) nanoparticles as efficient photocatalytic redox catalysts. *RSC Adv.*, 5(43), 34302–34313. https://doi.org/10.1039/C4RA17076H

18. Yang, Y. et al. (2017). Nitrogen-doped $TiO_2$(B) nanorods as high-performance anode materials for rechargeable sodium-ion batteries. *RSC Adv.*, 7(18), 10885–10890. https://doi.org/10.1039/C7RA00469A
19. Nguyen, T. K. A. et al. (2021). The effect of graphitic carbon nitride precursors on the photocatalytic dye degradation of water-dispersible graphitic carbon nitride photocatalysts. *Appl. Surf. Sci.*, 537, 148027. https://doi.org/10.1016/j.apsusc.2020.148027
20. Palanisamy, G. et al. (2021). Construction of magnetically recoverable ZnS–$WO_3$–$CoFe_2O_4$ nanohybrid enriched photocatalyst for the degradation of MB dye under visible light irradiation. *Chemosphere*, 273, 129687. https://doi.org/10.1016/j.chemosphere.2021.129687
21. Chalastara, K. et al. (2020). Tunable composition aqueous-synthesized mixed-phase $TiO_2$ nanocrystals for photo-assisted water decontamination: Comparison of anatase, brookite and rutile photocatalysts. *Catalysts*, 10(4), 407. https://doi.org/10.3390/catal10040407
22. Luttrell, T. et al. (2014). Why is anatase a better photocatalyst than rutile? - Model studies on epitaxial $TiO_2$ films. *Sci. Rep.*, 4(1), 4043. https://doi.org/10.1038/srep04043
23. Bernardini, C. et al. (2010). Photocatalytic degradation of organic molecules in water: Photoactivity and reaction paths in relation to $TiO_2$ particles features. *J. Photochem. Photobiol. A Chem.*, 211(2), 185–192. https://doi.org/10.1016/j.jphotochem.2010.03.006
24. He, X. & Zhang, C. (2019). Recent advances in structure design for enhancing photocatalysis. *J. Mater. Sci.*, 54(12), 8831–8851. https://doi.org/10.1007/s10853-019-03417-8
25. Náfrádi, M. et al. (2021). *Photocatalysis: Introduction, Mechanism, and Effective Parameters.* Cham: Springer International Publishing, 3–31. https://doi.org/10.1007/978-3-030-77371-7_1
26. Coleman, H. M. et al. (2007). Degradation of 1,4-dioxane in water using $TiO_2$ based photocatalytic and $H_2O_2$/UV processes. *J. Hazard. Mater.*, 146(3), 496–501. https://doi.org/10.1016/j.jhazmat.2007.04.049
27. Aziztyana, A. et al. (2019). Optimisation of methyl orange photodegradation using $TiO_2$ -zeolite photocatalyst and $H_2O_2$ in acid condition. *IOP Conf. Ser. Mater. Sci. Eng.*, 546 042047. https://doi.org/10.1088/1757-899X/546/4/042047
28. Zhu, H. et al. (2012). Effective photocatalytic decolorization of methyl orange utilizing $TiO_2$/ZnO/chitosan nanocomposite films under simulated solar irradiation. *Desalination*, 286, 41–48. https://doi.org/10.1016/j.desal.2011.10.036
29. Neppolian, B. et al. (2002). Solar/UV-induced photocatalytic degradation of three commercial textile dyes. *J. Hazard. Mater.*, 89(2), 303–317. https://doi.org/10.1016/S0304-3894(01)00329-6